Contract No.:

This manuscript has been authored by Savannah River Nuclear Solutions (SRNS), LLC under Contract No. DE-AC09-08SR22470 with the U.S. Department of Energy (DOE) Office of Environmental Management (EM).

Characterization of Uranium Tetrafluoride (UF_4) with Raman Spectroscopy

(Eliel Villa-Aleman* and Matthew S. Wellons)

Savannah River National Laboratory
Aiken, SC, 29808

Abstract

The Raman spectrum of uranium tetrafluoride (UF_4) is unambiguously characterized with multiple Raman excitation laser sources for the first time. Across different laser excitation wavelengths, UF_4 demonstrates 16 distinct Raman bands within the 50-400 cm^{-1} region. The observed Raman bands are representative of various F-F vibrational modes. UF_4 also shows intense fluorescent bands in the 325 – 750 nm spectral region. Comparison of the UF_4 spectrum with the ZrF_4 spectrum, its crystalline analog, demonstrates a similar Raman band structure consistent with group theory predictions for expected Raman bands. Additionally, a demonstration of combined scanning electron microscopy (SEM) and in situ Raman spectroscopy microanalytical measurements of UF_4 particulates shows that despite the inherent weak intensity of Raman bands, identification and characterization are possible for micron-sized particulates with modern instrumentation. The published well characterized UF_4 spectrum is extremely relevant to nuclear materials and nuclear safeguard applications.

Keywords: Uranium Tetrafluoride, Nuclear Forensics, In Situ SEM/Raman Spectroscopy

Introduction

The uranium fluorides (U_xF_y) are of industrial, governmental, and academic interest; primarily dependent on their application within the nuclear fuel cycle for both uranium chemical and enrichment processes.[1] UF_6 is a primary product from the chemical processing of uranium concentrates and ore into U feedstock for processing via centrifuge or gaseous diffusion enrichment. UF_4 is similarly important as a reaction intermediate in the fluorination process up to UF_6 and post enrichment chemical processing into uranium oxides and metal for reactor fuel fabrication. UF_5 has a minor role in the molecular laser isotope separation (MLIS) process as an enriched photolysis product, but otherwise is largely absent from industrially relevant processes.[2,3] Other known uranium fluorides, such as UF_3 and U_4F_9 are either purely of academic interest only and/or esoteric intermediate species, and all with minimal published study.[4-6]

The completeness of the chemical and structural characterization of the uranium fluorides mostly reflects their industrial application; with UF_6 by far the most completely characterized. The crystalline structure (solid phase), IR-Raman spectra, ^{19}F NMR shifts, and many other thermodynamic and kinetic properties of UF_6 are well known.[7,8] The other industrially relevant pentafluoride and tetrafluoride materials have a similar level of basic characterization such as known crystal structures, but are generally less well studied.[9,10] Although there is some parity in the level of knowledge between these three industrially relevant uranium fluorides, UF_4 stands alone as the only one for which detailed Raman bands have neither been unambiguously characterized or modeled in silico. The Raman spectra of UF_6, α-UF_5 and β-UF_5 solids have been well characterized and a summation of previous efforts has been published by Armstrong et al.[11] Density functional theory calculations of UF_4 to predict Raman spectral bands have likely

not been performed due to the challenges of modeling relativistic unpaired electrons (U^{4+} compared to U^{6+}) in current common basis sets.[12,13] This gap in UF_4 spectral properties is particularly acute as Raman spectroscopy measurements are a convenient and straightforward characterization technique for industrial processing as well as nuclear safeguards and nuclear forensic methods focused on identification of particulate species.[14-16]

In particular, nuclear forensics represents an application where Raman analysis can provide unique probative data of chemical speciation in a timely fashion. The non-destructive nature of Raman analysis makes it well suited for the characterization of special nuclear material forensic samples from throughout the fuel cycle; including the uranium and plutonium fluorides. Additionally unlike most traditional nuclear forensics techniques capable of analyzing single particulates (e.g. scanning electron microscopy or secondary ion mass spectrometry) Raman spectroscopy can provide chemical speciation information, allowing unambiguous identification. In addition to the technical data that is reported here, the efforts to characterize the Raman bands of the uranium fluorides validates the experimental design and models before moving on to the considerably more complex and difficult to handle Pu system.

Experimental

UF_4 and ZrF_4 were purchased from International Bio-Analytical Industries, Inc., and from Stem Chemicals Inc., respectively. Both chemicals were stored within active temperature and humidity controlled storage chambers (<10% relative humidity) to minimize contact with atmospheric water. The commercial UF_4 material consists of particles with spheroid morphology with dimensions that ranged from few microns up to 30 microns in diameter. The material has a vibrant green color consistent with UF_4 and purity was confirmed by powder XRD to verify material phase, see Fig. S1 (Supporting Information). A peak pattern consistent with known UF_4 was demonstrated and no other crystalline materials were detectable.[17] The purity of ZrF_4 was confirmed by powder XRD. A peak pattern consistent with known ZrF_4 was demonstrated and no other crystalline materials were detectable.

The X-ray diffraction (XRD) measurements were acquired using a Rigaku Ultima IV powder X-ray diffractometer with a multi-sample changer attachment. X-rays were produced from a copper target at 40 kV and 44 mA. Scattered X-rays were detected using a D/teX Ultra semi-conductor detector with a Cu Kβ filter, with the tube/detector operated in the focusing beam (Bragg Brentano) method. On the incident side of the beam, the divergence slit was set at 2/3° and the divergence height limit slit at 10 mm while the scattering slit was set at 8.0 mm and the receiving slit was open on the diffracted side of the beam. The sample substrate was a 1 inch silicon disk cut along the (510) crystal plane to minimize background reflections. Paraffin wax was used to secure the UF_4 powder on the substrate. The 2θ scan range was from 10 - 60° at a scan rate of 1.0° per minute. Measurements were performed with a stationary sample holder. XRD scans were analyzed with Rigaku PDXL instrument software. A qualitative analysis was performed using a peak search to match the experimental XRD pattern to the International

Center for Diffraction Data (ICDD) database of crystal and powder X-ray spectra using the peak intensity and peak position.

Micro-Raman spectra were acquired on two separate commercial Raman spectrometers. Spectra were collected on a LabRAM HR800 UV (Horiba Jobin-Yvon) and InVia (Renishaw) Raman spectrometers. The LabRAM microscope is equipped with a Newton electron multiplier charge-coupled device (EMCCD) (Andor 970N-UVB) detector with a 1600 x 200 pixel array; 16 microns pixel resolution. Most of the UF_4 experiments were conducted by binning the spectral array with a factor of two. The Andor detector was cooled to -95°C with the help of a water chiller. Labspec 5.78 software was used to control the spectrometer and detector. The software was also used to conduct data manipulations.

The excitation laser wavelengths for the LabRAM included λ = 325, 458, 488, 514, 633 and 785 nm. The laser beams were delivered to the sample through three different pathways in the LabRAM spectrometer. The laser sources included continuous wave (CW) lasers (Ar ion, HeNe, HeCd and diode). Five gratings tailored for different spectral regions (ultraviolet, visible and near-infrared) and with different groove density for different resolutions are available for the use with the spectrometer. Two gratings are installed in the spectrometer turret although gratings are easily replaced for the required work. A 600 and an 1800 g/mm grating were used in the visible spectral range. A 3600 g/mm blazed at 300 nm was used with the 325 nm laser. The spectral content of the laser beam was cleaned with a bandpass filter. Ultrasteep long pass edge filters acquired from Semrock, Inc were used to interrogate the vibrational spectra as close as 50 cm^{-1} of the laser excitation line. The laser power used in these experiments ranged from 100 µW to 3 mW. The laser intensity at the sample was controlled with neutral density filters and the microscope objective selection (primarily 50x, or 40x for ultraviolet light only). Laser power, microscope objective, pixel binning, grating and wavelength spectral region (fluorescence background) contributed to the integration time used during the acquisition of the Raman spectra. The integration time varied from few seconds to several hours for a high signal to noise ratio. For each integration time, at least two spectra were co-added to remove the contribution of cosmic rays to the spectra.

Micro-Raman spectra were also collected on a Renishaw InVia Raman spectrometer coupled with two excitation lasers consisting of a diode source single mode λ = 785 nm, 50 mW, and Ar ion λ = 514 nm, 50 mW, lasers. The laser power used in these experiments ranged from 100 µW to 3 mW. The laser intensity at the sample was controlled with neutral density filters and the microscope objective selection (primarily 100x). The InVia possesses automated beam steering optics, motorized components (Rayleigh slit; entrance slit; pinhole, diffraction gratings (either 1200 g/mm and 1800 g/mm)), 100 cm^{-1} Raman edge filters, plasma line rejection filters, and a UV-enhanced deep depletion (UVDD) CCD detector.

Electron microscopy and energy dispersive spectroscopic analysis of the UF_4 samples were conducted on a field emission Carl Ziess Supra 40VP Scanning Electron Microscope (SEM), and

an Oxford Xmax 80 mm^2 Energy Dispersive Spectrometer (EDS) detector operated by the Oxford Inca software. Attached to the chamber of the Supra-40 SEM is a Renishaw brand in situ optical microscope called the Selective Chemical Analyzer (SCA). The SCA allows in situ Raman measurements by extending excitation laser sources into the SEM and returning photon signals back to the InVia spectrometer hardware via fiber optics and a lens/mirror assembly. Raman spectra collected via the SCA were taken with both the 514 and 785 nm excitation laser sources attached to the InVia.

Discussion

Several attempts have been published on the characterization of UF_4 Raman bands within the past 50 years. In 1970 Krasser et al reported the vibrational spectrum and force constants of UF_4 and the Raman spectrum using a 50 mW HeNe laser (λ = 632.8 nm).[18] Raman bands were identified at 180, 340, 420 and 614 cm^{-1} corresponding to a tetrahedral molecular symmetry. This work was subsequently discredited by Goldstein et al in 1975 who examined spectra from UF_4-isostructural compounds (ZrF_4, HfF_4, and CeF_4) and postulated a three dimensional polymeric structure of for these molecules instead of the simplistic tetrahedral symmetry.[19] Goldstein et al opined that the apparent simplicity of the spectrum measured by Krasser et al arose from several overlapping bands and was not consistent with Raman spectra from the isostructural compounds. Goldstein et al unsuccessfully attempted to measure the UF_4 Raman spectrum with the Kr ion laser excitation source, λ = 647.1 nm, but material decomposition hindered meaningful characterization. Additional challenges arose in the characterization of the isostructural compounds as the effort failed to identify the Raman spectrum of CeF_4 and only a few Raman bands of HfF_4 spectrum due to strong fluorescence background. It was the successful characterization of the polymeric and complex Raman spectrum of ZrF_4 which provided evidence contrary to Krasser et al previously reported UF_4 spectrum.

For our study, six laser excitation lines were chosen to conduct Raman spectroscopy and validate the UF_4 polymeric structure. The objective of using several lasers in the identification of UF_4 Raman spectrum was to separate Raman bands from the fluorescence background. Laser lines at 325, 458, 488, 514, 633 and 785 nm were selected with the availability of ultrasteep edge filters capable of measurement of Raman bands as close as 50 cm^{-1} from the laser excitation in consideration. Although a search for Raman bands was conducted in the 50 to 1000 cm^{-1} spectral region, it became clear that Raman bands were primarily present below 400 cm^{-1}. Most work was confined to the 70 to 650 cm^{-1} spectral region based on our preliminary work and computational modeling of the Raman spectrum by Goldstein et al.[19] Long integration times (in some cases greater than four hours) at low laser intensities (< 2 mW) were necessary to improve S/N ratios of the spectra and to avoid material decomposition for some laser wavelengths. Assignment of probable Raman bands was accomplished by aligning the spectra acquired with the different laser lines and confidence in a particular assignment was achieved when bands were present in two or more spectra acquired with different lasers.

Fig. 1 shows the Raman spectrum of UF_4 acquired with seven different laser excitation sources between the two Raman spectrometers utilized; a total of five different excitation wavelengths. The intensity of the Raman spectra is arbitrary and was modified to ease presentation of the data into a single figure. The slope of the baseline in the spectra has been maintained in the figure for clarity on the luminescence background. Fluorescence background is an integral contributor to the noise in the spectrum. Raman spectra with an intense fluorescence background require long integration time to achieve a spectrum with clearly distinguishable UF_4 bands. The spectrum acquired with the 325 nm laser line was a significant challenge since the Raman spectrum was at the pinnacle of the fluorescence band and therefore with the largest noise. Raman spectra acquired with the 458, 488 and 514 nm laser lines were much cleaner and easier to analyze. In contrast to the Ar ion laser lines, the 633 nm (HeNe) laser line was located on the slope of a fluorescence band and extraction of a coherent Raman spectrum was almost impossible (not shown). The best spectra for band assignment analysis were acquired with the 514 and 785 nm laser lines. In particular Fig. 2 shows the UF_4 Raman spectrum acquired with the 514 nm laser line with labels for 16 Raman bands where the same bands were observed with the 785 nm excitation laser.

A tabulated list of the 16 Raman bands of UF_4 is illustrated in Table 1. Table 1 does not include few weak shoulder bands present in Fig. 2. As ZrF_4 is isostructural with UF_4, a comparison of their general vibronic structure is useful. ZrF_4 Raman bands measured in our laboratory are also presented in Table 1. The complexity of both UF_4 and ZrF_4 Raman spectra agree with Goldstein's original interpretation of polymeric structure. UF_4 is a monoclinic crystal species with the space group C2/c (C_{2h}, no. 15; Z=12); group theory analysis of isostructural compounds results in 42 potential Raman bands.[19] The calculation can be simplified by considering the fluorine atoms only due to the relative large mass of uranium atom compared to the fluorine atom. In this context the potential number of bands is reduced to 37.[19] The concept of pseudosymmetry was used to predict a total of twenty-one fluorine atom translations.[19] Although the UF_4 spectrum is not understood at this time, the number of bands measured in our work is consistent with theory; clearly shows the complexity and the extensive number of translations as predicted by Goldstein.

Fig. 3 shows the spectra (fluorescence and Raman) acquired with different excitation lines. The selection of the wavelength can induce large changes in the emission spectra as illustrated by the laser excitation at 458, 488 and 514 nm. The spectra suggest multiple sources for emission and most likely with different emission lifetimes. The Raman spectrum for the 325 nm laser excitation line was located on top of the fluorescence band. A closer look at the emission spectra observed with the 458, 488 and 514 nm laser excitation sources clearly shows that the Raman spectral region is significantly separated from the fluorescence band maximum. The reduced fluorescence background in the Raman spectral region resulted in a better S/N ratio. The best S/N ratio for the Raman spectra was acquired with the 514 nm excitation line (LabRam microscope). In contrast to the separation of the Raman spectral region and the fluorescence

band maximum observed with the 458, 488 and 514 nm laser lines, the intense emission background observed with the 633 nm laser line overwhelmed the Raman spectrum. Finally, although the fluorescence intensity was weak with the 785 nm laser line, the Raman scattering was also extremely weak with this excitation wavelength and most spectra were convoluted with fringes from optical etalonning (constructive and destructive interference pattern). Although the contribution of the fringes to the spectra was variable, significant distortion was observed in many spectra. Since the time these experiments were conducted, a new Andor detector (DU146A-LDC-DD) with fringe suppression technology was installed in the second port of the LabRAM microscope. The new detector with a wedged window and AR coatings optimized at 900 nm and using deep-depletion technology virtually eliminated optical etalonning from the spectra. The signal to noise ratio for the Raman spectra acquired with this detector (not shown) was significantly better than the broadband EMCDD detector used in this study. In contrast to the LabRAM microscope with the older version of the EMCCD detector, the detector in the InVia Raman microscope system equipped with a 1200 g/mm grating did not show the fringes in the spectrum. The main peaks of the UF_4 Raman spectrum were present in both Raman microscope systems. A cooling/heating stage was used to cool the UF_4 sample to -190 °C in an attempt to improve the spectral separation between the fluorescence and Raman bands but, unfortunately, no improvement in the S/N ratio of the Raman spectrum was observed (not shown).

To better validate UF_4 Raman spectral measurements an isostructural compound, ZrF_4, was characterized via several excitation sources (λ_{ex} = 458, 488, 514 and 785 nm) and the two different Raman microscope systems. In contrast to the 514 nm laser excitation line which produced significant fluorescence background, Raman spectra with high S/N ratios were acquired with the 457, 488 and 785 nm laser excitation wavelengths. Some similarities in peak position agree between this work and those previously recorded by Goldstein et al.[19] A total of 16 Raman bands were measured in this work at 73.8, 81.5, 90.7, 114.4, 130.3, 167.0, 201.6, 213.3, 253.3, 291.0, 319.7, 341.5, 372.2, 469.5, 499.5 and 564.0 cm^{-1} for ZrF_4. Additional bands might be located between the Raman bands and on the higher energy side shoulder of the 564 cm^{-1}. Goldstein et al reported Raman bands at 80, 90, 110, 163, 178, 198, 222, 260, 345, 391, 407, 425, 484, 505, and 655 cm^{-1}. Goldstein et al also examined the spectra of isostructural compounds (HfF_4 and CeF_4) to show the polymeric structure caused by fluorine bonding. Except for ZrF_4, fluorescence overshadowed the Raman spectrum in HfF_4 and CeF_4. Although the number of ZrF_4 Raman bands between this work and the previous effort are similar there is clearly a mismatch between the spectra. A possible explanation for the discrepancies in spectra may be partial hydrolysis of ZrF_4 in previous efforts; forming zirconium oxyfluorides in ambient conditions. All ZrF_4 materials utilized in this work were stored in environmentally (i.e. <10% relative humidity) controlled chambers and samples prepared in sealed containers with transparent quartz windows.

In this work, trace hydrolysis may have occurred in either the UF_4 and/or ZrF_4 systems on the material surface despite environmentally controlled sample storage. Likely particulate surfaces contain some trace quantities of absorbed water, however all characterization methods demonstrated signals (diffracted x-rays, U/F/O emitted x-rays, and Raman spectra for XRD, SEM/EDS, and Raman spectroscopy, respectively) consistent with a single species identified as UF_4. Additionally all three methods probe a similar depth into this type of material due to the physics of photon, XRD, and electron penetration/absorbance for the various energy sources utilized. We approximate that the three analytical techniques penetrate UF_4 materials, at most, a few microns in depth.

Unlike other previous UF_4 measurements, the Raman spectra acquired at different wavelengths demonstrate a multitude of Raman bands < 400 cm^{-1}. A weak band might be present at 605 cm^{-1}. The data do not support the presence of additional bands outside this spectral region. Ho et al reported a spectrum from a "UF_4" sample provided by the IAEA (λ_{ex} = 785 nm) with prominent bands around 860 and 400 cm^{-1} which were attributed to UF_4.[20] The spectrum most likely represented a combination of aging and decomposition products. The band located around 860 cm^{-1} was most likely due to a uranyl compound such as uranyl fluoride.[11] Pointurier et al used the 514 nm laser line to study UF_4 Raman spectroscopy and a "band" located at 914 cm^{-1} was assigned to UF_4.[21] The "band" was not confirmed with other laser wavelengths and may have represented anhydrous uranyl fluoride.[11] Unfortunately, the S/N ratio of the spectrum was poor and did not resolve the true Raman spectrum of UF_4 present in the 50 to 605 cm^{-1} region. A similar report of a 914 cm^{-1} Raman band for UF_4 was produced by Pidduck et al but since no spectra were published no conclusions can be made within this effort.[22] It is worth note, that within a publically available report by Lipp et al, UF_4 Raman bands acquired via excitation lasers at λ = 488 and 514 nm measuring Raman bands at 448 and 470 cm^{-1} within a diamond anvil cell measurements at high pressures (47 kbar) were demonstrated.[23] However these results are not directly compared with the spectra available in the literature due to the extreme pressures of the experiments and no spectra collected at standard temperature and pressure were provided.

The technology available to Krasser et al in the late 60's, although state-of-the-art at that time, was insufficient to deal with the complicated weak Raman spectrum of UF_4 in a fluorescent background.[18] Krasser et al assigned four broad bands in the Raman spectrum to UF_4. The intensity of their Raman spectrum decayed "exponentially" from the laser line. The attributes of the spectrum suggest significant laser scattering in the spectrometer and scattering contribution to the spectrum. Although the experimental work was not clearly described, the HeNe laser (633 nm) with a 50 mW power most likely decomposed the UF_4 material. Decomposition of UF_4 was observed in our work with the 785 nm laser line at powers less than 5 mW with a 100x objective. The decomposition of the UF_4 caused by the 785 nm laser could be followed with Raman spectroscopy using the 514 nm of the Ar^+ laser.

Challenges of the early studies into vibrational spectra of UF_4 were likely hindered by many instrumentation challenges including poor photon transmission throughput, poor light collection

efficiency from sample, low yield quantum efficiency detectors, and ultrasteep band pass filters. Additionally these instrumentation challenges were complicated by undesirable UF_4 chemical properties including intense fluorescence, weak Raman scattering from uranium-fluorine (U-F) bonds, and complications of fluorine-fluorine (F-F) bonding and its effect on the group symmetry. However, this effort demonstrates that UF_4 Raman spectral collection is possible, if time consuming, with current optics technologies such as high light throughput single-based spectrographs, high efficiency laser line bandpass filters, ultrasteep long pass edge filters in combination with high numerical aperture, and CCD detectors with high quantum yield and multichannel collection. Unfortunately beyond use of an additional Raman enhancement mechanism, such as surface enhanced Raman spectroscopy (SERS), the spontaneous Raman scattering of UF_4 is weak and can only be compensated by careful measurements. Future experimenters are advised to maximize laser power at sample while minimizing sample damage and utilizing long duration integration times to achieve identifiable spectral bands (100-1000s).

Demonstration and characterization of now known spectral features of UF_4 Raman bands can be directly applied to various fields, in particular nuclear safeguards. Identification of nuclear material particulates is increasingly relevant to nuclear safeguards applications focused on detection and characterization of uranium-bearing materials released through the course of various nuclear and chemical processes.[16] Traditionally the characterization techniques for these safeguards applications involve (computer-controlled SEM) CCSEM and/or SIMS or the Lexan method (fission tracks) to find uranium-bearing particles within an environmental matrix and characterize their elemental and/or isotopic composition. Although one can potentially infer chemical species from elemental measurements neither method can provide clear chemical speciation identification, particularly differentiating between various uranium oxides (e.g. UO_2, UO_3, U_2O_5, U_3O_8, etc.) or uranium-fluorine containing materials (e.g. UF_4, UF_5, UO_2F_2, etc.). FTIR, micro XRF, and micro Raman are all suitable techniques for characterization of uranium particulates but micro Raman is the only one capable on much smaller (<20 μm) sized features.[24] In particular, the use of a combined SEM and in situ Raman probe (e.g. SCA) allows the convenient combination of CCSEM searching and subsequent micro Raman analysis without the need for multi-instrument coordination.[25]

Equipped with the knowledge from table top instruments for the UF_4 Raman bands positions, particles with dimensions at and below 20 microns were analyzed with an SEM equipped SCA Raman probe. Previous efforts have utilized the SCA to characterize various uranium oxides in situ within a SEM, but none have published UF_4 particulate measurements.[26,27] Multiple particles were analyzed in this work and representative Raman spectra are shown in Fig. S2 (Supporting Information). Fig. S3 (Supporting Information) shows a representative UF_4 spheroidal particle with a dimension of 21 μm in diameter and with an F/U ratio consistent with UF_4. Two excitation lasers (514 and 785 nm) were used to characterize the UF_4 spectrum for this particle in series and although the Raman bands are present with the 514 nm laser measurement, the presence of fluorescent background made it extremely difficult to detect the Raman bands. In

contrast, the Raman spectrum acquired with the λ_{ex} = 785 nm laser eliminated most of the fluorescence and clearly shows Raman bands at 131.4, 170.6, 254.7, and 299.5 cm^{-1} (see Fig. S2); consistent with the table top Raman instruments. These measurements show that it is possible to identify the molecular structure of a given particle and provide a pathway to differentiate other particles containing U and F such as UO_2F_2.[28]

The differences in measurements between this work and previous particle UF_4 characterization efforts are not completely understood. Pointurier et al did not specifically identify particulate sizes for the UF_4 but stated "only particles in the size range of a few μm to a few tens of μm were studied".[21] Particulates analyzed within this effort all fall within these size regimes. Instead likely integration time and/or laser fluence at the sample for previous efforts was insufficient to capture distinct UF_4 Raman bands in the < 500 cm^{-1} spectral region. Spectra shown in Fig. S2 (Supporting Information) were collected with a single integrated scan of 1000 s at 50% (i.e. 1 mW at the sample) and 100% (i.e. 3 mW at the samples) of the maximum laser fluence of the λ_{ex} = 514 and 785 nm lasers, respectively. These parameters are in stark contrast to those reported by Pointurier et al where 3 spectra of 20s each, from 100 cm^{-1} to 2000 cm^{-1} were collected per particle measurement within a standard optical microscope setup with laser power set to 1% (i.e. 0.5 mW) and 0.5% (i.e. 1.5 mW) for the λ_{ex} = 514 and 785 nm lasers, respectively. The characterization of UF_4 particles is possible with a SCA but longer duration integrations and higher laser power are required for unambiguous spectra.

Concerns regarding thermal stability of the UF_4 features with extended measurement integration, time and high laser power proved to be a nonissue. SEM imaging shown in Fig. S3 (Supporting Information) of a UF_4 particle post Raman analysis for sequential λ_{ex} = 514 and 785 nm laser measurement by the parameters described above, clearly shows none of the morphological changes typically seen with laser induced decomposition. Further characterization with EDS, Fig. S3 (Supporting Information), demonstrates typical presence of U and F whose intensities were similar to other particles not subjected to micro Raman analysis. Note that no attempt was made to establish a quantitative U/F ratio due to the known challenges of X-ray absorption and fluorescence corrections for the EDS of micron sized features.[29] Particle damage only occurred when the λ_{ex} = 514 nm laser was set at 100% maximum laser fluence (i.e. 2 mW at the sample) or when EDS measurements with duration greater than a 10-15 seconds were attempted (probe current 500 pA; accelerating voltage 20 kV).

Conclusion

Multiple UF_4 Raman spectra have been proposed since 1970 by several authors. The contradicting results by different researchers is likely the combination of the inherently weak UF_4 Raman spectrum, lack of modern instrumentation, and the presence of a strong fluorescence background for many laser excitation sources. Since fluorescence can affect the baseline of the Raman spectrum significantly, "bands" were identified as Raman bands as long as they were present in two or more spectra from differing laser excitation sources. Across different laser

excitation wavelengths, UF_4 demonstrates 16 distinct Raman bands within the 50-400 cm^{-1} region which are representative of various F-F vibrational modes. Within the excitation laser sources tested, the most useful for identification were the λ_{ex} = 514 and 785 nm, depending on spectral region of interest. Since Raman scattering depends on the fourth power of the excitation wavelength and the photon efficiency of the CCD detector, the Raman scattering is higher for 514 nm laser excitation line versus 785 nm laser excitation line. A balance between fluorescence background and detection sensitivity is required at all times. The λ_{ex} = 514 nm used with the LabRAM microscope equipped with the Andor detector (no AR coatings) offered better S/N but exhibited intense fluorescence in the spectral region > 500 cm^{-1}. In contrast to the LabRAM microscope, the better response of the InVia CCD detector for the λ_{ex} = 785 nm and the low fluorescence in this spectral region made it a formidable wavelength for the detection of UF_4. The λ_{ex} = 785 nm offers adequate spectra for conventional spectrometers without low band pass filters but due to reduced S/N will likely require increased integration times for sufficient spectra resolution.

Despite weak Raman scattering, UF_4 particulates can be identified with correlation microscopy methods and we have demonstrated that successful chemical detection can be accomplished in situ (i.e. SCA). This, in combination with standard SEM (automated or otherwise) methods to locate uranium-bearing particulates, provides a powerful tool for nuclear safeguards and forensics particulate characterization. The UF_4 Raman spectra theoretical characterization still remains and further efforts will focus on correlation of DFT modeling with UF_4 spectra as new uranium basis sets become available. Additional future effort will also focus on extension of this effort into Raman spectroscopy characterization of other uranium and plutonium fluorine-containing compounds relevant to nuclear safeguards and forensics.

Acknowledgments

The authors wish to thank Michael Summer and Ross Smith for their contributing efforts on the collection of SEM images and Raman spectra of UF_4; Sheldon Nichols for his contributing efforts on the collection of XRD data; Dr. Lindsay Roy on her consultations regarding the current state of computational modelling of uranium materials. This work was funded by the Office of Defense Nuclear Nonproliferation Research and Development within the U.S. Department of Energy¹s National Nuclear Security Administration and the Savannah River National Laboratory, Laboratory Directed R&D funding (LDRD) project #SRNL-2015-00142.

References

[1] B. Morel, S. Chatain, in *Comprehensive Nuclear Materials*, (Eds: R. Konings, T. Allen, R. Stoller, S. Yamanaka), Elsevier, Amsterdam, **2012**, *2*, pp. 197-215.

[2] M. Hirasawa, Y. Kuga, T. Seto, K. Okuyama, K. Takeuchi, *Appl. Phys. A: Mater. Sci. Process.* **2002**, *74*, 513.

[3] M. Hirasawa, Y. Kuga, T. Seto, K. Okuyama, K. Takeuchi, *Appl. Phys. A: Mater. Sci. Process.* **1999**, *68*, 75.

[4] M. Karbowiak, J. Drozdzynski, *Chem. Phys.* **2007**, *340*, 187.

[5] J. C. Warf, *U.S. Atomic Energy Commission*, **1958**, *TID-5290*, 81.

[6] P. G. Eller, A. C. Larson, J. R. Peterson, D. D. Ensor, J. P. Young, *Inorg. Chim. Acta* **1979**, *37*, 129.

[7] P. W. Wilson, *Rev. Pure Appl. Chem.* **1972**, *22*, 1.

[8] P. E. Magnelind, A. N. Matlashov, P. L. Volegov, M. A. Espy, *IEEE Trans. Appl. Supercond.* **2009**, *19*, 816.

[9] J. C. Taylor, A. B. Waugh, *J. Solid State Chem.* **1980**, *35*, 137.

[10] W. H. Zachariasen, *Acta Crystallogr.* **1949**, *2*, 296.

[11] D. P. Armstrong, R. J. Jarabek, W. H. Fletcher, *Appl. Spectrosc.* **1989**, *43*, 461.

[12] D. A. Pantazis, F. Neese, *J. Chem. Theory Comput.* **2011**, *7*, 677.

[13] M. Dolg, X. Cao, *Chem. Rev.* **2012**, *112*, 403.

[14] Y. Ranebo, N. Niagolova, N. Erdmann, M. Eriksson, G. Tamborini, M. Betti, *Anal. Chem.* **2010**, *82*, 4055.

[15] D. Donohue, A. Ciurapinski, J. Cliff, F. Rudenauer, T. Kuno, J. Poths, *Appl. Surf. Sci.* **2008**, *255*, 2561.

[16] *IAEA Department of Safeguards Long-Term R&D Plan, 2012-2023*, STR-375, International Atomic Energy Agency, Vienna, **2013**.

[17] *PDF 4 Database*, International Centre for Diffraction Data, Newtown Square, PA, **2015**, Card No #01-082-2317.

[18] W. Krasser, H. W. Nuernberg, *Spectrochim. Acta, Part A* **1970**, *26*, 1059.

[19] M. Goldstein, R. J. Hughes, W. D. Unsworth, *Spectrochim. Acta, Part A* **1975**, *31A*, 621.

[20] D. M. L. Ho, A. E. Jones, J. Y. Goulermas, P. Turner, Z. Varga, L. Fongaro, T. Fanghaenel, K. Mayer, *Forensic Sci. Int.* **2015**, *251*, 61.

[21] F. Pointurier, O. Marie, *Spectrochim. Acta, Part B* **2010**, *65*, 797.

[22] A. J. Pidduck, M. R. Houlton, G. M.Williams, D. L. Donohue, Micro-analytical Characterization of Uranium Particles in Support of Environmental Sampling for Safeguards, in 47th *Annual Meeting Proceedings of the Institute of Nuclear Materials Management*, Nashville, Tennesee, July 16-20, 2006, Institute of Nuclear Materials Management, Northbrook, Illinois, **2006**, 181, pp 1-8.

[23] M. J. Lipp, Z. Jenei, J. P. Klepeis, W. J. Evans, *Raman Investigation of The Uranium Compounds U_3O_8, UF_4, UH_3 and UO_3 Under Pressure at Room Temperature*, LLNL-TR-522251, Lawrence Livermore National Laboratory, 2011.

[24] J. R.Schoonover, F. Weesner, G. J. Havrilla, M. Sparrow, P. Treado, *Appl. Spectrosc.* **1998**, *52*, 1505.

[25] U. Admon, D. Donohue, H. Aigner, G. Tamborini, O. Bildstein, M. Betti, *Microsc. Microanal.* **2005**, *11*, 354.
[26] F. Pointurier, O. Marie, *J. Raman Spectrosc.* **2013**, *44*, 1753.
[27] E. A. Stefaniak, F. Pointurier, O. Marie, J. Truyens, Y. Aregbe, *Analyst* **2014**, *139*, 668.
[28] E. A. Stefaniak, L. Darchuk, D. Sapundjiev, R. Kips, Y. Aregbe, R. V. Grieken, *J. Mol. Struct.* **2013**, *1040*, 206.
[29] J. Goldstein, D. E. Newbury, D. C. Joy, C. E. Lyman, P. Echlin, E. Lifshin, L. C. Sawyer, J. R. Michael, *Scanning Electron Microscopy and X-ray Microanalysis*, Springer, New York, **2003**.

"Characterization of Uranium Tetrafluoride (UF_4) via Raman Spectroscopy" figures and captions

Table 1: Raman spectral bands of UF_4 and ZrF_4.

UF_4 Raman Bands	ZrF_4 Raman Bands
59.4 (s)	73.8 (vw)
66.8 (m)	81.5 (vw)
78.9 (s)	90.7 (vw)
91.0 (w)	114.4 (w br)
101.3 (w sh br)	130.3 (w br)
107.2 (w)	167.0 (v w)
115.9 (w)	201.6 (w br)
131.4 (s)	213.3 (w br)
148.5 (sh)	253.3 (vw)
170.4 (m)	291.0 (vw)
197.3 (w)	319.7 (w sh)
255.8 (m sh)	341.5 (m sh)
296.1 (s)	372.2 (m)
322.4 (sh)	469.5 (m sh)
360.8 (sh)	499.5 (vs)
603.6 (w)	564.0 (m)

v=very, s=strong, m=medium, w=weak, br=broad, sh=shoulder

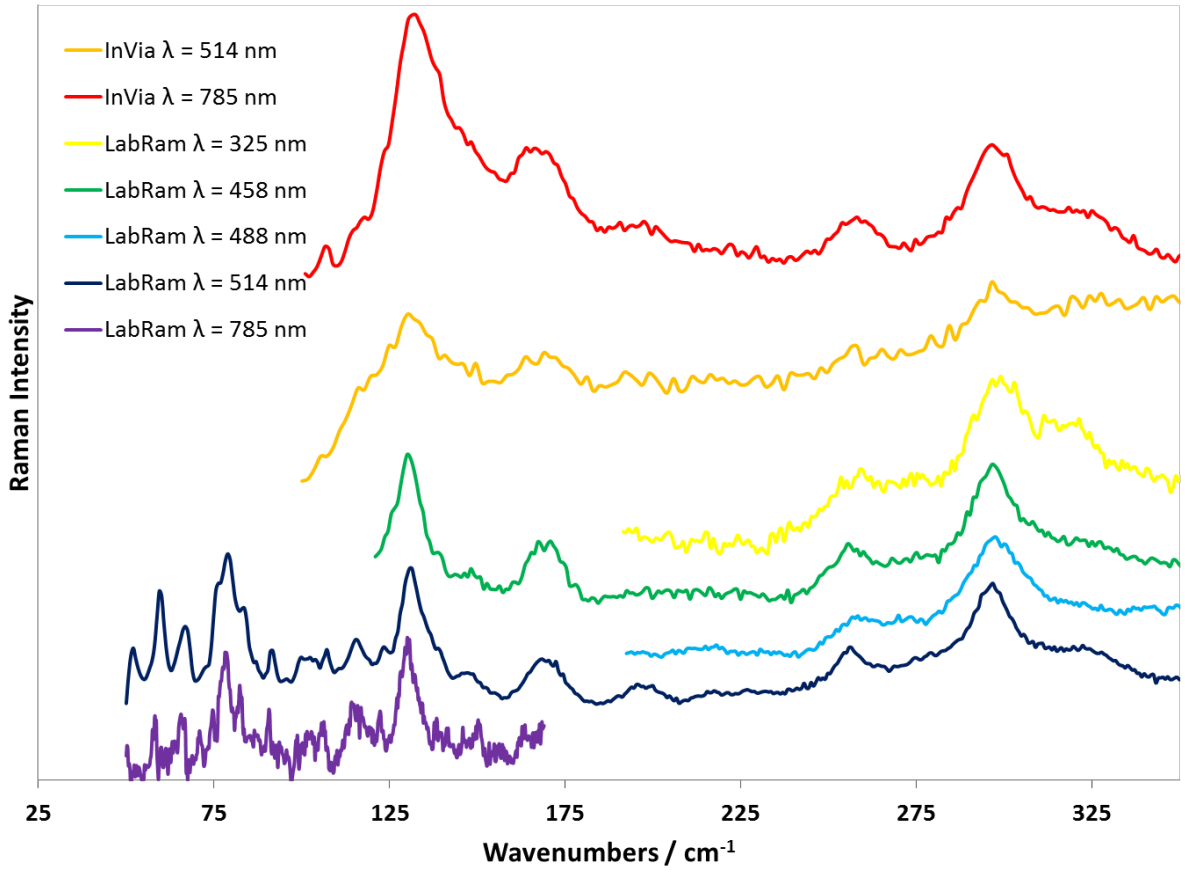

Figure 1: UF_4 Raman spectra acquired with five excitation laser lines on the Horiba Jobin-Yvon LabRam HR800 UV and two excitation laser lines on a Renishaw InVia spectrometer.

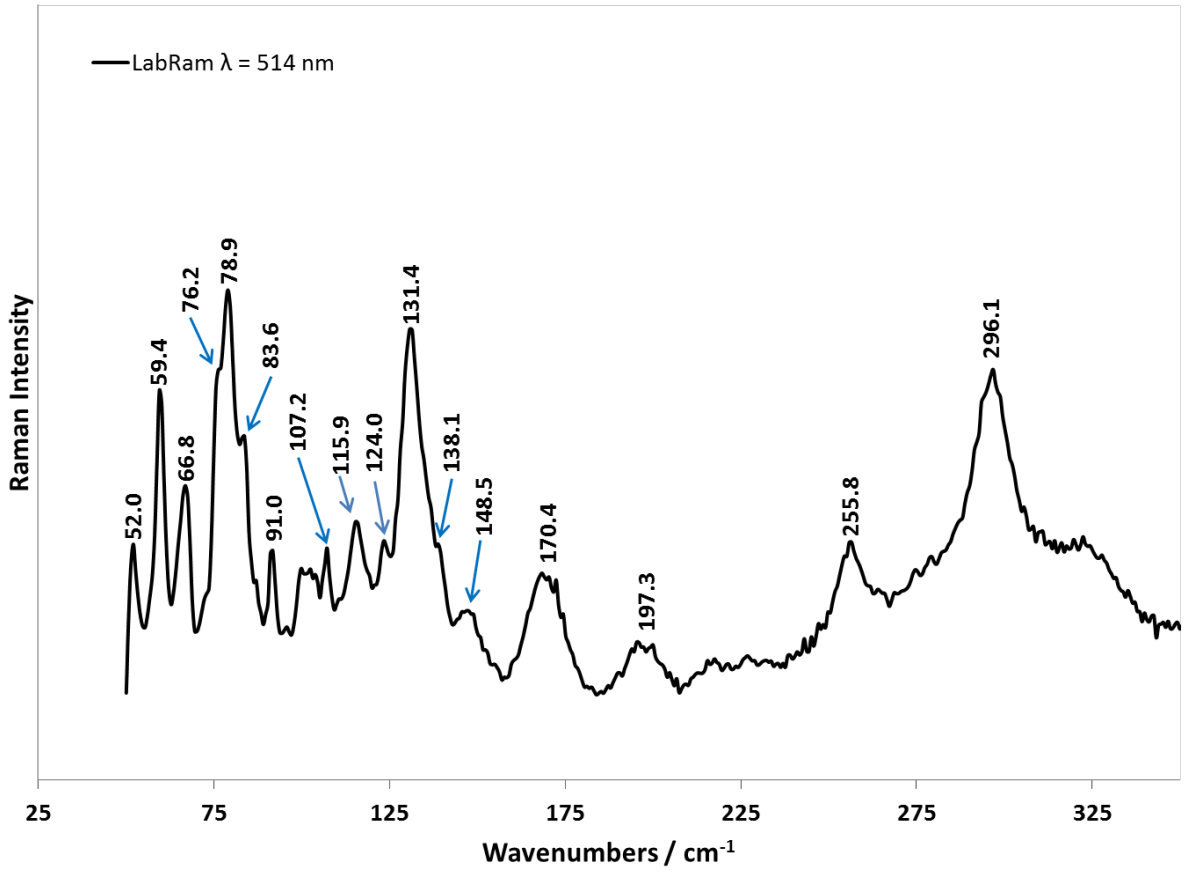

Figure 2: Select Raman bands identified as UF_4 acquired with a 514 nm excitation laser line on the Horiba Jobin-Yvon LabRam HR800 UV Raman spectrometer.

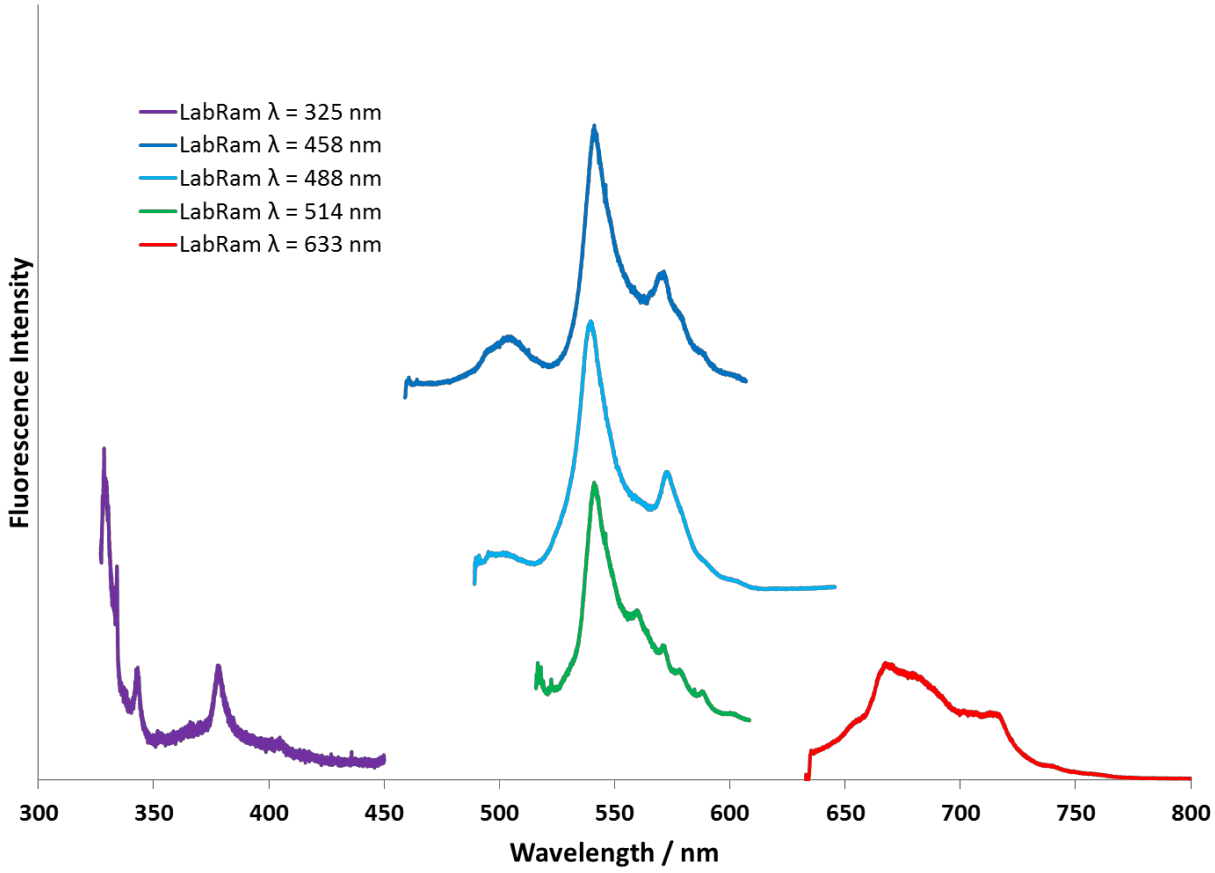

Figure 3: Fluorescence spectra of UF_4 from 300-800 nm acquired with five excitation lines collected on the Horiba Jobin-Yvon LabRam HR800 UV Raman spectrometer.

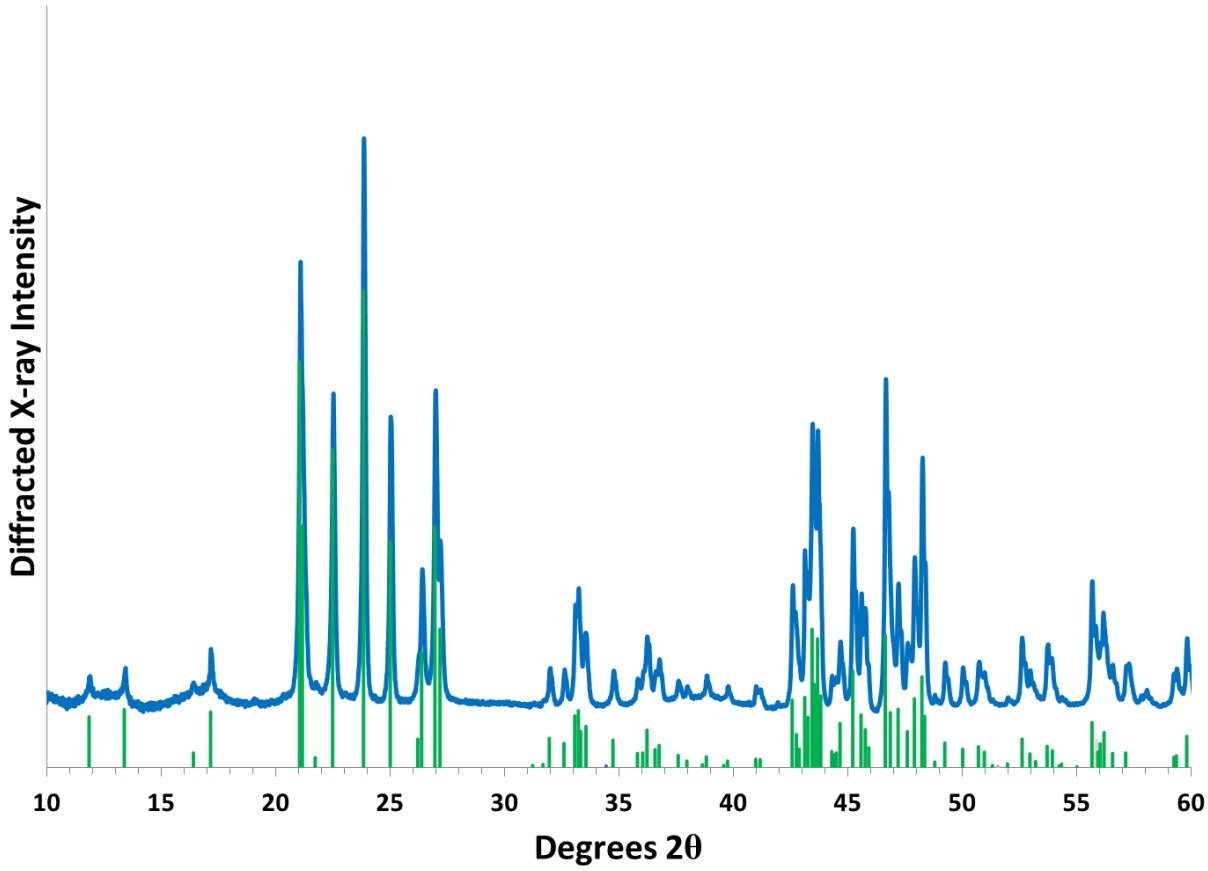

Figure S1: XRD scan of commercial UF_4 powder (blue) with corresponding line pattern shown for a UF_4 reference: PDF #01-082-2317 (green).

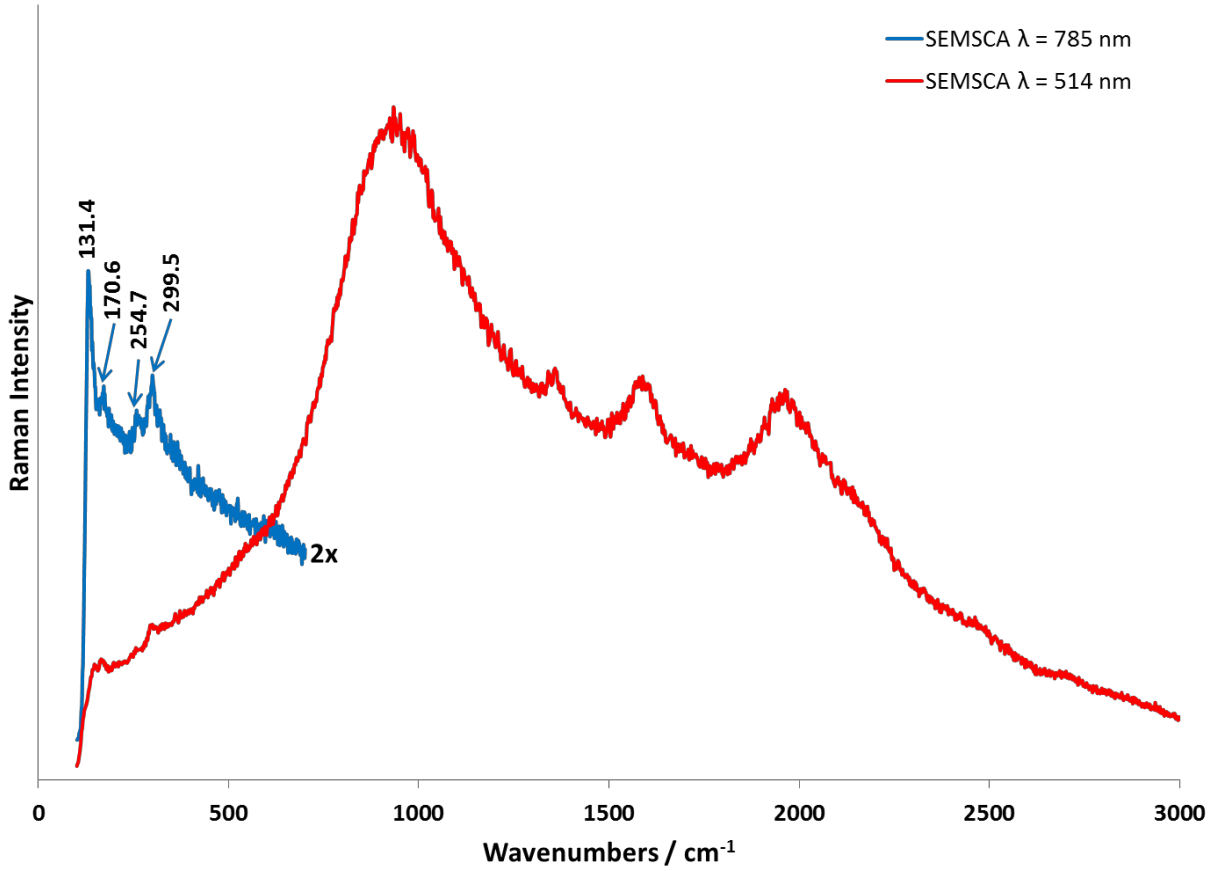

Figure S2: UF_4 Raman spectra acquired with two excitation laser lines on the Renishaw InVia SCA attachment coupled to a Ziess SUPRA 40VP SEM of an approximately 20 µm diameter UF_4 particle.

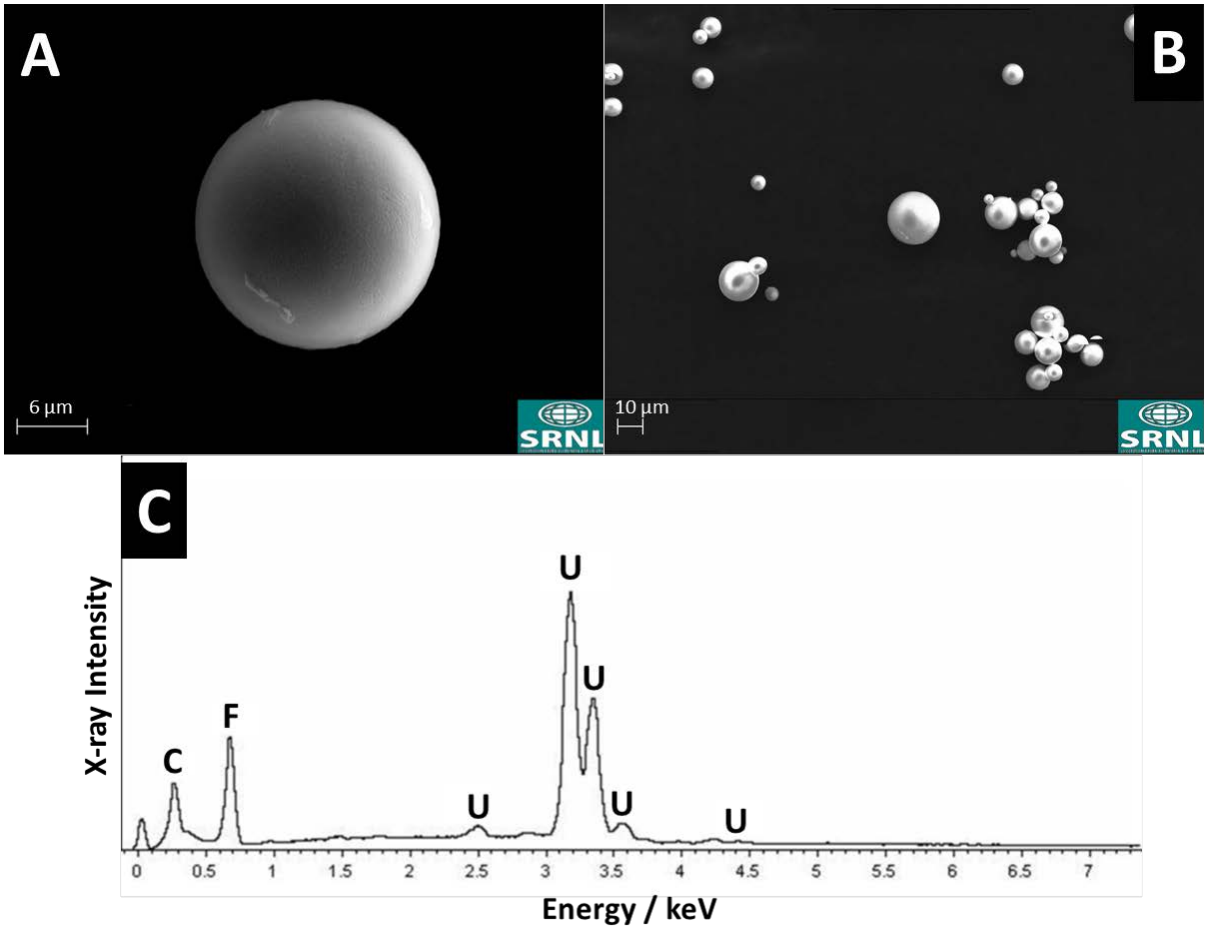

Figure S3: SE SEM images of a UF_4 particle (diameter approximately 20 µm) chosen for microanalytical characterization; (A) single particulate at 2200x magnification post Raman spectroscopy measurements with both 514 and 785 nm laser excitation lines, (B), same central particulate with surrounding particles at 500x magnification, (C) EDS spectra post laser irradiation.